Affinely Adjustable Robust Volt/Var Control for Distribution Systems with High PV penetration

Seyyed Mahdi Noori Rahim Abadi, Ahmad Attarha, Paul Scott, and Sylvie Thiébaux

***Abstract*—We propose two novel two-stage Volt/Var control schemes based on the affinely adjustable robust counterpart (AARC) methodology, to mitigate the over-voltage issues caused by integration of photovoltaic panels into distribution systems. To cope with different grid code requirements, our first approach formulates the unused capacity of residential inverters to provide reactive power support based on the real power deviation, while the second approach formulates them based on voltage magnitude deviation. In the first stage of both schemes, we make central measurements throughout the network to determine a linear function, mapping the operating point deviations to the reactive power of inverters. In the second stage, the local controllers use the provided linear functions to determine the required reactive power to keep the voltages within the safe limits. Unlike similar approaches, voltage limit constraints are directly incorporated into the AARC problem, preventing the second stage controllers from unnecessarily use of reactive powers. We compare the performance of our schemes using a Monte-Carlo simulation with four other existing techniques on a real-world 27-bus and the IEEE 906-bus LV feeders. Our simulations show that our approaches decrease the real power loss, reactive power usage, and line congestion compared to the other Volt/Var control schemes.**

***Index Terms*—Distribution system, DER integration, Volt/Var control, Affinely adjustable robust.**

I. Introduction

IN THE last decade, massive uptake of residential photovoltaic (PV) panels has led to new challenges in operating distribution systems [1]. Peak PV generation typically happens simultaneously with relatively low residential load consumption, which can cause overvoltage, especially in weak low voltage (LV) networks. Traditional approaches to controlling voltage, i.e., using capacitor banks, on-load tap changers, and step voltage regulators were designed to control voltage fluctuations caused by slow changes in demand throughout a day [2]. These methods are not adequate to respond to the fast and often synchronized variations of PV systems and would present an expensive solution when installed extensively throughout the distribution system [3]. The utilization of reactive power support capability of smart inverters presents a low-cost alternative that can provide fast and dynamic reactive power response [4].

In order to get an effective and flexible response at the network-wide level, the installed residential inverters need to be coordinated in some way. In the literature, there are a variety of techniques, which can be broadly classified based on their communication requirements as centralized, decentralized, and local [5]. Centralized approaches bring the inverter / meter measurements to a central location, make a control decision, and then relay that information back to the inverters in the field. They have the potential to make the best decisions, due to their system-wide perspective, but they run into computation and communications problems in highly volatile settings where the controllers need to be coordinated very frequently (in a matter of seconds) [6]. By foregoing some solution quality, decentralized approaches can mitigate the computational and single point of failure problems that a centralized approach has. However, the convergence of such approaches is highly dependant on the convexity of the problem, making them less attractive in real-time voltage control applications [7]. Unlike centralized and decentralized approaches, a local control approach only relies on local measurements available to the inverter. However, because a local controller lacks a system-wide perspective, its actions can be far from optimal [8].

To overcome the shortcomings of these approaches, in this paper, we propose to use a combined local and centralized approach. The idea is to benefit from both the system-wide coordination of centralized approaches and the fast response of local approaches. We use a timescale decomposition technique [9] to combine the two approaches and form a two-timescale scheme. This should be intuitive as there exist slow-acting and fast-acting voltage control devices working together in distribution systems. In these approaches, a discrete controller periodically takes measurements throughout the network and sends corrective adjustments to the local layer. Then in real-time, the local controller takes recourse actions after the uncertainty is realized [7]–[10]. Using such a scheme, we can extend the period between two consecutive updates of the centralized layer, making it practical for use in large distribution systems.

Moreover, we make use of the affinely adjustable robust counterpart (AARC) methodology introduced in [11] to ensure that the voltage limits are not violated between two consecutive updates. This is achieved by factoring in the impact of uncertainty in the centralized layer when the controller parameters are calculated and communicated to the local layer. In AARC, similarly to a linear feedback controller, the output of the controllers can be constantly updated as the uncertain parameters are revealed. In our context, such an AARC approach is in the spirit of a combined centralized and local control approach, where the system-wide decisions (known as "here-and-now" values) are made through a centralized optimization, while the "wait-and-see" control action are made locally to tune the "here-and-now" values.

Recently, the application of (AARC), or equivalently, linear decision rules (LDR) in voltage control has been investigated in the literature [12], [10], [7]. In [12], the coordination of

Authors are with the College of Engineering and Computer Science, The Australian National University (ANU), Canberra, Australia. (mahdi.noori@anu.edu.au, ahmad.attarha@anu.edu.au, paul.scott@anu.edu.au and sylvie.thiebaux@anu.edu.au)

residential battery energy storage systems is formulated as an AARC problem and solved using a distributed optimization algorithm. A linear decision rule is assigned to each battery relating uncertain household real power consumption to battery charge / discharge response. [10] proposed using LDR for adjusting the reactive power of multiple inverters in response to local changes in real power injection. The parameters in the decision rules are obtained based on linearized power flow equations. This work is extended in [7] by presenting a closed-form solution to the AARC of Volt/Var problem.

Note that the above literature designs the decision rules without actually incorporating the voltage limits in their model. The decision rules in [7] and [10] are designed to keep the voltages close to (ideally the same as) the voltage references. Thus, there is no guarantee that their results lie within the voltage safe limits. Also, [7] and [10] use as much reactive power as they can to keep the voltages the same as the reference value. This not only leads to over-consumption of reactive power, which can potentially lead to an increase of real power losses, but also (as we show in Section V) can increase line congestion in the distribution system.

To address these shortcomings, in this paper, we propose two novel Volt/Var control schemes based on AARC to keep voltages within predefined limits using residential inverters. To cope with different grid code requirements, our first approach formulates the reactive power of inverters based on their real power deviation, while the second approach formulates them based on voltage magnitude deviation. In the first stage of both schemes, we propose to decouple the AARC of the Volt/Var problem into convex quadratically constrained programming (QCP) and linear programming (LP) sub-problems. The QCP sub-problem is a centralized optimal power flow with the objective of minimum real power loss subject to voltage limit constraints. The LP sub-problem is used to optimize the linear relation between the inverters' reactive power and real power deviation in the first scheme, and voltage magnitude deviation in the second scheme. The second stage is a local feedback controller that determines the inverter reactive power, using the provided linear functions and local measurements.

Numerical analysis is used to compare our proposed methods with the existing Volt/Var control techniques in the literature, including two purely local control approaches, i.e., fixed droop based Volt/Var control suggested by IEEE standard 1547 [13], and incremental droop control proposed in [14]; also, the state-of-the-art in Volt/Var control based on AARC proposed in [7], and the optimal solution that has knowledge of the eventual realization of uncertainty. Our analysis shows that factoring the actual network voltage limits into the decision-making process will significantly decrease excess reactive power usage and real power loss in the system. It should be noted that with increasing voltage issues in distribution systems, it is predicted that new ancillary service markets will emerge to incentivize consumers to provide reactive power support [15]. In such a situation, the excessive use of reactive power puts an unnecessary economic burden on the distribution system operator. Another strength of our approach is that the two AARC formulations facilitate the integration of such control approaches with existing regulations and grid code requirements. For example the German grid code mandates that the reactive power of residential inverters be a function of real power [16], and the Australian grid code mandates that the reactive power of residential inverters be a function of voltage magnitude [17]. The major contributions of this work are:

- an AARC of Volt/Var problem that formulates the inverters' real-time reactive power response as a linear function of voltage magnitude;
- a novel formulation that improves the state-of-the-art solution [7] to the Volt/Var problem which uses AARC to formulate the inverters' real-time reactive power response as a linear function of their real power deviation. We modify the formulation by incorporating the voltage and inverter limit constraints directly in the formulation at early stages of developing the linear function. Our simulations show that our approach, compared to [7], leads to less voltage violations and significantly decreases inverter's reactive power usage, network real-power loss, and line congestion;
- a Monte-Carlo based comparison between our proposed approaches and 4 alternative Volt/Var techniques in small and large scale distribution systems. Our experiments demonstrate that not only our approaches can keep the voltages inside the accepted limits for a wider range of scenarios, but also significantly decrease the reactive power usage, real power loss, and line congestion, compared to the alternative approaches.

We must point out that we leave the assessment of more detailed load and inverter models, such as considering ZIP load models [18] and the harmonics injected by the non-linear loads [19] and PV inverters [20], [21] to future works. Also, while our proposal is compatible with the wide-area hierarchical voltage control scheme used in transmission systems [22]–[24], it is different in that it aims to coordinate multiple inverters to guarantee safe voltage limits in the area of interest in the LV network, rather than coordinating devices in an interconnected multi-voltage level system. We leave the integration of our proposed approach with higher voltage control schemes to a future work.

The rest of this paper is organized as follows. In section II the problem formulation and a short summary of the AARC technique are presented. In section III our proposed methods are introduced. A short summary of other Volt/Var techniques are presented in section IV, and simulation results are reported in section V. Scalability to large distribution systems is investigated in section VI. Finally, section VII concludes this paper.

II. Affinely Adjustable Robust Counterpart

The real power injected into networks by PV inverters increases the voltage at the common coupling point. As demonstrated in [25], the voltage rise problem can be mitigated through reactive power absorption from the grid. Fortunately, the remaining capacity of the inverters can be effectively used for this purposes (i.e., consuming reactive power). However, properly coordinating and controlling numerous inverters across the distribution system is a challenging task.

To overcome this challenge, we use the idea of adjustable robust control, introduced by Ben-Tal and et al. in [11]. However, before presenting our approach, we briefly provide an overview of the adjustable robust control methodology to provide the required setup on which we build our approach in Section III.

Ben-Tal and et al. originally designed their algorithm to deal with the uncertainty in real-time. For their purpose, they introduced an AARC approach in which the variables are modelled as linear functions of the uncertain parameters. They showed that the AARC approach is not only computationally tractable, but also that it is significantly less conservative compared to conventional Robust Counterpart approaches. Their affine function can be written as follows:

$$X(\zeta) := X^{opt} + \alpha\zeta, \tag{1}$$

where $X(\zeta)$ is the control variable, comprising a non-adjustable part X^{opt} and an adjustable part $\alpha\zeta$. ζ is the uncertain parameter in the original problem, while X^{opt} and α are the decision variables in the robust counter part problem. Fixing X^{opt} and α in real-time operation allows the variable X to affinely tune itself to the volatility of the uncertain parameter ζ. In other words, similarly to a linear feedback controller, the value of X can be constantly updated as the uncertain parameters are revealed.

III. Proposed Approach

In this section, we propose an affinely adjustable robust counterpart of the Volt/Var problem based on real powers (AARBP) and an affinely adjustable robust counterpart of the Volt/Var problem based on voltage magnitude (AARBV). Fig. 1 shows an overview of our proposed two-stage process. The two stages in our proposed approach are differentiated from each other using the black-dotted line, and the data required to initialize the first stage is shown in the ovals on top. In the first stage of our control approaches, we obtain the inverter parameters, which are then communicated to the inverters through a communication channel. Since both of our proposed approaches are linear, they remain computationally tractable for networks with large numbers of PV inverters. We assume we have a reliable communication infrastructure that allows us to send the smart inverter parameters at regular intervals. Such communication infrastructure is an essential feature of smart grids, and various research and standards have been published to help realize it [26]. In the second stage, using the updated parameters and local measurements, the inverter reactive power set-points are calculated. The real power set-points are obtained using the maximum power point tracker (MPPT) included in the PV system to maximize power extraction under all conditions (note that the MPPT functionality is not the focus of our work). A regular inverter feedback controller is then used to achieve and maintain these set points on the AC side.

Our first stage optimization is done periodically in the background (in our simulation, we solve the optimization problem every 5 minutes), while the local controllers in the second stage work in real-time. We update the controller parameters when we have a new output from our optimization problem. The two blocks in Fig. 1 are detailed in the following subsections.

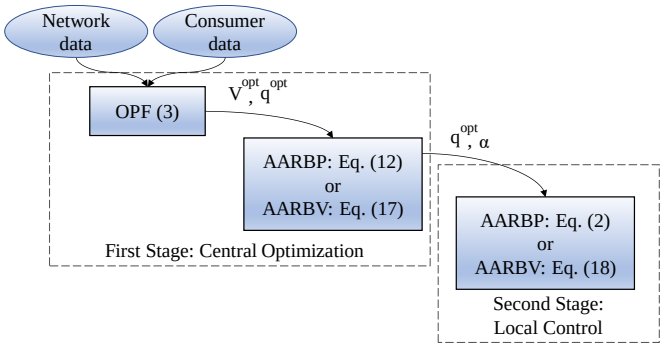

Fig. 1. High-level structure of our proposed central-local control system.

A. AARBP

In line with the German grid code, coordination of the reactive power contribution of PV inverters can be achieved using a linear relation between their real and reactive powers. To do this, we consider that measurements are made periodically throughout the network. Then, using these measurements, an optimal power flow (OPF) with the objective of minimizing real power loss is solved to obtain the ideal reactive power contribution of each inverter. Finally, to deal with operating point deviations in each period, we suggest to use a linear relation between the change in reactive power contribution and the real power deviation from the value measured at the start of the period by each inverter as follows:

$$q_i^{inv}(\Delta p_i^{inv}) = q_i^{opt} + \alpha_i \Delta p_i^{inv}, \tag{2}$$

where q_i^{inv} is the inverter reactive power connected to bus i, q_i^{opt} is the optimal reactive power obtained from the OPF at the beginning of each period, Δp_i is the real power deviation from the measurement, and α_i is the slope of the linear decision rule. The affine function (2) includes a bi-linear term $\alpha_i \Delta p_i^{inv}$, and thus the resulting AARC problem would be difficult (if at all possible) to solve. However, the uncertain parameter Δp_i^{inv} has a bounded polyhedral uncertainty set and provided that the rest of the problem is linear, we can use duality theory to obtain a linear AARC model. Unfortunately, this is not the case in our problem as our approach features a nonlinear OPF model. To resolve this, we decoupled the problem into two subproblems. In the first one, we use a convex conic relaxed OPF model to calculate the values of q_i^{opt}. In the second one, we linearize the power flow equations about the OPF solution of the first stage. This two-stage approach has the benefit of both accounting for the nonlinear power flow equations, and a tractable AARC model.

1) How to obtain q_i^{opt}: We use the *Distflow* model to represent the power flow equations, as the *Distflow* formulation is well-suited for radial distribution systems with a tree structure, as shown in [27]. In the *Distflow* formulation, a power network is represented by a connected graph $\mathcal{G} = (\mathcal{V}, \mathcal{B})$, where each

node represents a bus and each edge represents a line or branch. $\mathcal{V} = \{1, ..., n\}$ denotes the set of buses with cardinality $|\mathcal{V}| = n$ and $\mathcal{B} \subseteq \mathcal{V} \times \mathcal{V}$ denotes the set of all branches and (i, k) or $i \to k$ represents a branch from bus i to bus k. For every bus $i \in \mathcal{V}$, let v_i denote the squared voltage magnitude. Also, let $P_i^{inj} = P_i^{inv} - P_i^{load}$ be the real power injected to the grid at bus i, and $Q_i^{inj} = Q_i^{inv} - Q_i^{load}$ be the reactive power injected to the grid at bus i. For every branch $(i, k) \in \mathcal{B}$, let $z_{ik} = r_{ik} + jx_{ik}$ denote the complex impedance of the line, and l_{ik} denote the squared current magnitude between bus i and bus k. It is also assumed that the substation voltage set-point v_0 is given. Moreover, the inverter capacity and voltage limit constraints are incorporated in the *Distflow* model. What follows is the OPF formulation:

$$\min \quad \sum_{(i,j)\in\mathcal{B}} r_{ij} l_{ij} \tag{3a}$$

$$P_j^{inj} = \sum_{k:j\to k} P_{jk} - (P_{ij} - r_{ij} l_{ij}) \qquad \forall j \in \mathcal{V} \tag{3b}$$

$$Q_j^{inj} = \sum_{k:j\to k} Q_{jk} - (Q_{ij} - x_{ij} l_{ij}) \qquad \forall j \in \mathcal{V} \tag{3c}$$

$$v_j = v_i - 2(r_{ij}P_{ij} + x_{ij}Q_{ij}) + (r_{ij}^2 + x_{ij}^2) l_{ij} \quad \forall (i,j) \in \mathcal{B} \tag{3d}$$

$$v_i l_{ij} \geq P_{ij}^2 + Q_{ij}^2 \qquad \forall (i,j) \in \mathcal{B} \tag{3e}$$

$$P_j^{inj} = p_j^{inv} - P_j^{load} \qquad \forall j \in \mathcal{V} \tag{3f}$$

$$Q_j^{inj} = q_j^{inv} - Q_j^{load} \qquad \forall j \in \mathcal{V} \tag{3g}$$

$$p_j^{inv^2} + q_j^{inv^2} \leq S_j^{max^2} \qquad \forall j \in \mathcal{V} \tag{3h}$$

$$v_j^{min} \leq v_j \leq v_j^{max} \qquad \forall j \in \mathcal{V}, \tag{3i}$$

where (3b)-(3g) denote the *Distflow* equations, (3h) enforces the inverter capacity constraint, and (3i) denotes the voltage limitations. Note that (3e) is a conic relaxed version of the original quadratic equality constraint. This is a tight relaxation as the objective function includes l_{ij}, which prevents excessive deviation from the equality (our simulations show that relaxing this constraint introduces less than 0.5% error).

2) How to obtain α_i: The variable α_i is used to deal with voltage deviations due to the uncertainties in inverter real powers. A linear relation between the voltage deviation, and deviations in real and reactive power of inverters can be obtained by linearizing the power flow equation about an operating point [28] as follows:

$$\Delta V_i = \sum_{k=2}^{n} K_{ik}^p \Delta p_k^{inv} + K_{ik}^q \Delta q_k^{inv} \qquad \forall i \in \mathcal{N} \tag{4a}$$

$$K_{ik}^p = \frac{\partial V_i}{\partial p_k^{inv}}, \quad K_{ik}^q = \frac{\partial V_i}{\partial q_k^{inv}}, \tag{4b}$$

where $\mathcal{N} = \mathcal{V} - \{1\}$ denotes the set of all buses expect the slack bus. Substituting $\Delta q_k^{inv} = \alpha_k \Delta p_k^{inv}$ from (2) into (4a), we can obtain the voltage deviations in terms of the uncertain parameter, i.e., real power of the inverter, as follows:

$$\Delta V_i = \sum_{k=2}^{n} (K_{ik}^p + \alpha_k K_{ik}^q) \Delta p_k^{inv}. \tag{5}$$

Remember that our goal here is to deal with uncertainties to prevent voltage violation. This can be formulated as follows:

$$V^{min} \leq V_i \leq V^{max}. \tag{6}$$

For any small changes around the operating point we can write the two equivalent linear equations:

$$V_i^{opt} + \Delta V_i \leq V^{max}, \quad V_i^{opt} + \Delta V_i \geq V^{min}, \tag{7a}$$

where V_i^{opt} is the voltage magnitude obtained from the centralized OPF at the beginning of each interval at bus i. Considering the linear decision rules, the voltage deviation term can be replaced with (5) as follows:

$$V_i^{opt} + \sum_{k=2}^{n} (K_{ik}^p + \alpha_k K_{ik}^q) \Delta p_k^{inv} \leq V^{max} \tag{8a}$$

$$V_i^{opt} + \sum_{k=2}^{n} (K_{ik}^p + \alpha_k K_{ik}^q) \Delta p_k^{inv} \geq V^{min}. \tag{8b}$$

We use a polyhedral uncertainty set to model the deviation of PV power from a forecast:

$$\Delta p_i^{inv} \in \mathcal{U} = [\Delta p_i^{min}, \Delta p_i^{max}] \tag{9a}$$

$$\Delta p_i^{min} \leq 0 \leq \Delta p_i^{max}. \tag{9b}$$

Such an uncertainty set notifies that the PV power can deviate from its forecast in either a positive or negative direction, which is representative of how PV power behaves in practice. We only consider the uncertainty in PV generation. This is in line with the state of the art [7] to enable us to compare our approach with the recent related works. Regarding the uncertainty of loads, since we run our optimization model and obtain the AARC control parameters every 5 minutes, at every run, we take the latest (most accurate) load forecast into account.

Now we can rewrite (8) as the following optimization problem. We consider the objective to be equal to the minimum of aggregated values of $|\alpha_i|$. The idea is to obtain the minimum aggregate change from the optimal reactive power values in all the buses that can keep the voltages in the accepted limits, for all operating point deviations. Also, to obtain practical values for α_i we consider the inverter capacity constraint.

$$\min \quad \sum_{i=2}^{n} \alpha_i^{aux} \tag{10a}$$

$$\text{(8a), (8b)} \qquad \forall i \in \mathcal{N} \tag{10b}$$

$$p_i^{inv^2} + q_i^{inv^2} \leq S_i^{max^2} \qquad \forall i \in \mathcal{N} \tag{10c}$$

$$\alpha_i^{aux} \geq \alpha_i, \quad \alpha_i^{aux} \geq -\alpha_i \qquad \forall i \in \mathcal{N}, \tag{10d}$$

where (10d) is used to linearize the absolute value of α_i in the objective function. To avoid repetition, these two constraints are not included in the formulations in the rest of this paper, instead only the absolute value over α_i is used. (10c) is a circle in (p_i^{inv}, q_i^{inv}) coordinates, which can be linearized using a set of linear equalities as follows:

$$(cos(\phi) + sin(\phi)) q_i^{inv} + (cos(\phi) - sin(\phi)) p_i^{inv} \leq \sqrt{2} S_i^{max} \quad \forall i \in \mathcal{N}, \forall \phi \in \mathcal{A}, \tag{11}$$

where $\mathcal{A} = \{0, \pi/m, 2\pi/m, ..., (2m-1)\pi/m\}$, and m is an arbitrary integer number. Considering the same box uncertainty set (9), and partitioning the real power of the inverter $P_i^{inv} = P_i^{inv_0} + \Delta P_i^{inv}$, we can obtain the affinely adjustable robust counterpart (AARC) of (10), using the duality technique used in [10] as follows:

$$\min \quad \sum_{i=2}^{n} |\alpha_i| \tag{12a}$$

$$V^{max} - V_i^{opt} \geq \sum_{k=2}^{n} \theta_{ik}^{'} \Delta P_k^{max} + \theta_{ik}^{''} \Delta P_k^{min} \tag{12b}$$

$$\theta_{ik}^{'} + \theta_{ik}^{''} \geq (K_{ik}^{p} + \alpha_k K_{ik}^{q}) \tag{12c}$$

$$\theta_{ik}^{'} \geq 0, \quad \theta_{ik}^{''} \leq 0 \tag{12d}$$

$$V_i^{opt} - V^{min} \geq \sum_{k=2}^{n} \lambda_{ik}^{'} \Delta P_k^{max} + \lambda_{ik}^{''} \Delta P_k^{min} \tag{12e}$$

$$\lambda_{ik}^{'} + \lambda_{ik}^{''} \geq -(K_{ik}^{p} + \alpha_k K_{ik}^{q}) \tag{12f}$$

$$\lambda_{ik}^{'} \geq 0, \quad \lambda_{ik}^{''} \leq 0 \tag{12g}$$

$$(cos(\phi) + sin(\phi)) q_i^{opt} + (cos(\phi) - sin(\phi)) p_i^{inv_0} + \gamma_{i\phi}^{'} \Delta P_i^{max} + \gamma_{i\phi}^{''} \Delta P_i^{min} \leq \sqrt{2} S_i^{max} \tag{12h}$$

$$\gamma_{i\phi}^{'} + \gamma_{i\phi}^{''} \geq (cos(\phi) - sin(\phi)) + \alpha_i (cos(\phi) + sin(\phi)) \tag{12i}$$

$$\gamma_{i\phi}^{'} \geq 0, \quad \gamma_{i\phi}^{''} \leq 0 \tag{12j}$$

$$j, k \in \mathcal{N}, \quad \phi \in \mathcal{A}, \tag{12k}$$

where $\theta_{ik}^{'}$, $\theta_{ik}^{''}$, $\lambda_{ik}^{'}$, $\lambda_{ik}^{''}$, $\gamma_{ik}^{'}$ and $\gamma_{ik}^{''}$ are dual variables. The convex quadratic problem (3) and linear problem (12) can be solved in polynomial time [29]. We used the *Gurobi* solver in our experiments.

B. AARBV

In this section we propose an AARC formulation of the Volt/Var problem, which is in line with the IEEE 1547 standard and the Australian grid code. Similar to the approach described in section III-A, we consider a two-stage approach with periodic measurement throughout the network. In the first stage, after solving OPF (3), the following linear decision rule based on the voltage magnitude is used to deal with operating point deviations in each period:

$$q_i^{inv}(\Delta V_i) = q_i^{opt} + \alpha_i \Delta V_i. \tag{13}$$

Substituting $\Delta q_i^{inv} = \alpha_i \Delta V_i$ from (13) to (4a), and considering the same objective as (10), we obtain the following optimization problem:

$$\text{(4a), (10a), (10d), (11)} \tag{14a}$$

$$\Delta q_i^{inv} = \alpha_i \Delta V_i. \tag{14b}$$

Constraint (14b) has a bilinear term, which makes (14) non-convex. Unfortunately, unlike in (10), the duality technique described in section III-A cannot be used directly to linearize the problem. Other relaxation techniques for bilinear terms, e.g., McCormick's relaxation [30], depend heavily on having tight variable bounds [31]. In fact, general relaxation of bilinear terms is an ongoing research topic in the field of optimization. In our case, since tight bounds on α_i is not available prior to solving (14), using McCormick's relaxation may produce poor results, which would degrade performance of the controller in the second layer. As an alternative, to solve problem (14) we propose approximating voltage deviation (5) with only the deviation in real power, i.e. ignoring how reactive power changes voltage in the network in the LDR phase. Then, the impact of reactive power on voltage is factored back in at the local control phase, by using (13) to change the reactive power at discrete points in time rather than continuously updating it. This is in the spirit that the inverter reactive powers are controlled to prevent voltage violation due to changes in real powers. This creates a time difference between the effects of real and reactive power changes in voltage deviation. The idea is to take benefit from the time difference to decouple the voltage deviation caused by changes in inverter reactive powers, from the deviations caused by real powers. The motivation behind this will be further explained later in the paper, after introducing the modified discrete version of the voltage-base linear decision rule (equation (18)). Applying this approximation we obtain the following optimization problem:

$$\text{(10a), (10d), (11)} \tag{15a}$$

$$\sum_{k=2}^{n} (K_{ik}^{p} \Delta p_k^{inv} + \alpha_k K_{ik}^{q} \sum_{j=2}^{n} K_{ij}^{p} \Delta p_j^{inv}) \leq V^{max} - V_i^{opt} \tag{15b}$$

$$\sum_{k=2}^{n} (K_{ik}^{p} \Delta p_k^{inv} + \alpha_k K_{ik}^{q} \sum_{j=2}^{n} K_{ij}^{p} \Delta p_j^{inv}) \geq V^{min} - V_i^{opt}. \tag{15c}$$

Simplifying (15) results in:

$$\min \quad \sum_{i=2}^{n} |\alpha_i| \tag{16a}$$

$$\sum_{k=2}^{n} (K_{ik}^{p} + \sum_{j=2}^{n} \alpha_j K_{ij}^{q} K_{jk}^{p}) \Delta p_k^{inv} \leq V^{max} - V_i^{opt} \tag{16b}$$

$$\sum_{k=2}^{n} (K_{ik}^{p} + \sum_{j=2}^{n} \alpha_j K_{ij}^{q} K_{jk}^{p}) \Delta p_k^{inv} \geq V^{min} - V_i^{opt} \tag{16c}$$

$$(cos(\phi) + sin(\phi)) q_i^{opt} + (cos(\phi) - sin(\phi)) p_i^{inv_0} + (cos(\phi) - sin(\phi)) \Delta p_i^{inv} + (cos(\phi) + sin(\phi)) \alpha_i \sum_{j=2}^{n} K_{ij}^{p} \Delta p_j^{inv} \leq \sqrt{2} S_i^{max}. \tag{16d}$$

Considering the same box uncertainty set (9), and the same duality technique as used in (12) we can obtain the following AARC for (16):

$$\text{(12a), (12b), (12d), (12e), (12g), (12h), (12j)} \tag{17a}$$

$$\theta_{ik}^{'} + \theta_{ik}^{''} \geq (K_{ik}^{p} + \sum_{j=2}^{n} \alpha_j K_{ij}^{q} K_{jk}^{p}) \qquad \forall i, k \in \mathcal{N} \tag{17b}$$

$$\lambda_{ik}^{'} + \lambda_{ik}^{''} \geq -(K_{ik}^{p} + \sum_{j=2}^{n} \alpha_j K_{ij}^{q} K_{jk}^{p}) \quad \forall i, k \in \mathcal{N} \tag{17c}$$

$$\gamma_{ij\phi}^{'} + \gamma_{ij\phi}^{''} \geq \alpha_i (cos(\phi) + sin(\phi)) K_{ij}^{p} +$$

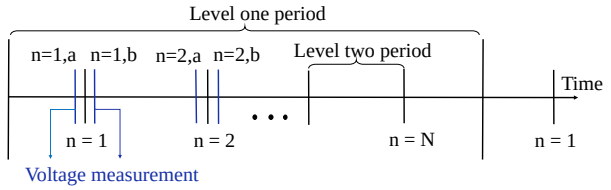

Fig. 2. A sample of the discrete time definition used in (18). The level one period is the time between two consecutive centralized adjustments, and the level two period is the time between two consecutive discrete decisions.

$$(cos(\phi) - sin(\phi)) \qquad \forall i = j \in \mathcal{N}, \forall \phi \in \mathcal{A} \quad (17d)$$

$$\gamma^{'}_{ij\phi} + \gamma^{''}_{ij\phi} \geq$$

$$\alpha_i(cos(\phi) + sin(\phi))K^p_{ij} \qquad \forall i \neq j \in \mathcal{N}, \forall \phi \in \mathcal{A}. \quad (17e)$$

Solving optimization problem (17) yields values for α_i. Now we introduce the discrete version of the voltage-base linear decision rule as follows:

$$q_i^{inv,n+1} = q_i^{inv,n} + \alpha_i(V_i^{n+1,a} - V_i^{n,b}), \qquad (18)$$

where n is an index for each discrete change in reactive power, and a and b represent voltage measurements made just before and after the n-th reactive power adjustment, as shown in Figure 2. An example is presented here to demonstrate, how based on (18) the reactive powers in each instance are calculated. To calculate the reactive powers at instance $n = 2$, the voltage is measured at $n = 2, a$. Then, it is compared with the voltage magnitude at $n = 1, b$, and based on (18) a new value for reactive power is obtained. After applying the calculated reactive powers, at $n = 2, b$ the voltage magnitudes are measured and stored to be used in the next instance. This process should be intuitive as it means the calculated values for reactive power at decision time n will not change at decision time $n + 1$, if the operating point has not changed since the actions made at n. Under such a scheme, the voltage deviation caused by changes in inverter reactive powers is decoupled from the deviations caused by real powers, which makes the approximation used in (15) possible. Note that this approach is practical under the assumption that changes in network operating point occur more slowly than the time required for the inverter to inject / absorb the calculated value, and measure the new voltage profile. This is a justifiable assumption as the time required for the inverters to do the above mentioned actions is in the order of hundreds of milliseconds, and the PV and load variations are generally in the order of tens of seconds [25].

C. Use of Auxiliary Variables

In general the Volt/Var problem with hard voltage and inverter capacity constraints may not always have a feasible solution regardless of the approach. In these circumstances we would still like to take an action that reduces the voltage violation by as much as possible. To achieve this we convert these to soft constraints by introducing auxiliary variables for the voltage limit constraints ((12b) and (12e)), and the inverter capacity constraints ((12h)). These auxiliary variables are then included in the objective function with large penalty coefficients.

IV. Alternative Techniques

In this section, the three alternative techniques for Volt/Var control, introduced in section I, are briefly summarized. These techniques along with the two proposed techniques, AARBP and AARBV, and the optimal solution considering perfect realization of uncertainty will be compared in section V.

A. Fixed Droop Based Volt/Var Control

This approach is suggested by IEEE standard 1547, where the reactive power of each inverter is calculated as follows:

$$q_i^{inv} = \begin{cases} \big[-\alpha_i(V_i - (V_i^{nom} - \epsilon_i))\big]_{q^{min}}^{q^{max}} & V_i < V_i^{nom} - \epsilon_i \\ 0 & V_i^{nom} - \epsilon_i \leq V_i \leq V_i^{nom} + \epsilon_i \\ \big[-\alpha_i(V_i - (V_i^{nom} + \epsilon_i))\big]_{q^{min}}^{q^{max}} & V_i < V_i^{nom} + \epsilon_i, \end{cases} \qquad (19)$$

where V_i^{nom} is the nominal voltage value, usually considered equal to one per-unit. $2\epsilon_i$ is the dead-band size, and α_i is the slope of the droop. Operator $[.]_{.^{min}}^{.^{max}}$ enforces the inverter reactive power capacity limit.

B. Incremental Droop Based Volt/Var Control

This approach is proposed in [14], where the reactive power of each inverter is calculated as follows:

$$q_{i,t+1}^{inv} = \begin{cases} \big[q_{i,t}^{inv} - \alpha_i(V_i - (V_i^{nom} - \epsilon_i))\big]_{q^{min}}^{q^{max}} & V_i < V_i^{nom} - \epsilon_i \\ 0 & V_i^{nom} - \epsilon_i \leq V_i \leq V_i^{nom} + \epsilon_i \\ \big[q_{i,t}^{inv} - \alpha_i(V_i - (V_i^{nom} + \epsilon_i))\big]_{q^{min}}^{q^{max}} & V_i < V_i^{nom} + \epsilon_i, \end{cases} \qquad (20)$$

where index $t \in \mathcal{T} = \{0, 1, .., T\}$ denotes the number of discrete time steps. This approach acts similar to an integral feedback controller, where the reactive power at each time step is a summation of the reactive power at previous time step and the deviation from a reference value.

C. LDR Based on Real Powers Proposed in [7]

In this approach the reactive power of each inverter is obtained using the following linear rule:

$$q_i^{inv} = q_i^{opt} + \alpha_i \Delta p_i^{inv}. \qquad (21)$$

Note that although both (21) and AARBP use the same linear decision rule, the optimization algorithm used to obtained the value of α_i is different. The main difference is that in [7] α_i is determined in a way to minimize the voltage deviation irrespective of the voltage limits. However, AARBP aims to determine α_i to keep the voltages inside the voltage limits.

V. Numerical Results and Discussion

We test the performance of the different methods using simulation on a real 27-bus underground LV feeder with $R/X \approx 2$ located in Hobart, Australia [4]. Three cases with different system operating points are considered for the comparison. In *Case 1* the voltage profile is well-below the voltage limits, and even in the worst case condition the voltage limits will not be

breached. In *Case 2* all the voltages at the measurement time are below the limits. However, under the worst case condition the voltage limits will be breached. In *Case 3* the network is operating at the limit, which means that there is at least one bus whose voltage magnitude is equal to the voltage limit at the measurement time. Therefore, any increase in real power injections would result in voltage violation.

We assume that measurements are made throughout the network every 5 minutes, and the resolution of PV data is one minute. In all of the cases, PV generation with uniform distribution between 0-4 kW is randomly assigned to each node. W.l.o.g., we assume that PV panels are installed at all nodes to account for a system with a rich PV penetration level. In subsection V-A a detailed result for one scenario, i.e., measurement followed by a change in the operating point, is presented for each case. In subsection V-C a Monte Carlo simulation is carried out. 250 scenarios are generated between the three cases. Then, each scenario is simulated for 4 minutes, with the decision rules / droops acting every one minute, resulting in a total of 1000 random operating points.

A. Detailed Results for One Scenario

Fig. 3 shows the voltage profile and reactive power usage of the inverters at each bus in the three cases using the different Volt/Var control schemes.

In *Case 1* since (even in the worst condition) the voltage limits will not be violated, ideally it is expected that control schemes make a slight change in response to the operating point deviation, to keep the real power loss at minimum possible. In both AARBP and AARBV approaches, the value that we obtained for α is equal to zero in all the buses. The reason is that the operating point deviation does not lead to any voltage violation and thus, there is no need to any change in reactive powers in real-time to guarantee that voltages are within the limits. We can see in Fig. 3.d that the results of AARBP and AARBV is almost equal to the optimal solution. On the other hand, the AARC approach of [7] overuses the reactive power resources to keep all voltages at the measurement value (i.e., overusing the reactive power for an unnecessary requirement). Moreover, since the Inc. droop approach keeps all the voltages below 1.02 p.u., as plotted, it over-absorbs more reactive power than necessary.

In *Case 2* the measured values for PV generation indicates that none of the voltages are initially beyond their limits. However, since in some possible realisations of uncertainty over the next 4 minutes the voltage limits can be breached, α in AARBP and AARBV have negative values to absorb reactive power if real power injection increases. It can be seen in Fig. 3.e that AARBV has a better performance compare to other techniques and uses much less reactive power while keeping the voltage magnitudes inside the limit.

In *Case 3* the initial values for PV generation is in a way that at least in one bus voltage magnitude is beyond its predefined limit. Interestingly, we see that the results from AARC of [7] and now act very similarly, unlike in the previous cases. This happens in almost all the other random scenarios that we generated for case 3. This can be explained by observing (12). Since there is at least one bus whose voltage magnitude is equal to the limit, the value of $V^{max} - V_i^{opt}$ is equal to zero for that bus. So in turn the solver in (12) tries to minimize the voltage deviation in that bus to prevent the big penalty of having non-zero values for the soft voltage constraints. Therefore, the objective function of AARBP and AARC [7] will be close to each other. Moreover, we can see that in both schemes voltage violation occurs. In general for the extreme *Case 3* there are some scenarios where AARBV fails to keep the voltages inside the limits. We suggest an extension to AARBP and AARBV to deal with extreme *Case 3*, which will be introduced in subsection V-B.

B. Further Improvement in AARBP and AARBV to Handle Extreme Cases

We propose a further improvement to AARBP and AARBV by limiting the reactive power only to negative values, i.e. absorption, when extreme operating conditions occur such as *Case 3*. It is possible to automatically distinguish these extreme conditions from the other cases prior to running the AARC step by comparing the value of V_i^{opt} from solving the OPF with the voltage limits. Note that positive values for reactive power in some buses can help to decrease total real power loss. This is because the reactive power consumption of lines and loads can be sourced locally from inverters rather than needing to come from the upstream network, reducing current flow throughout the entire system. By applying this improvement, we are foregoing the ability to reduce losses in extreme cases to keep voltages inside the limits in more scenarios. Fig. 4 shows the voltage profile and the reactive power usage under AARBP and AARBV in the same operating point as chosen in Fig. 3.f. It can be seen that the voltages are brought to the limits under both schemes using their improved versions.

C. Average Results Over a Thousand Operating Points

Fig. 5 shows the average of real power loss and reactive power usage relative differences between the optimal solution and other approaches, over the thousand operating points. It can be seen that AARBP and AARBV significantly use less reactive power compared to the other techniques. This can be economically beneficial from the distribution system operator's perspective, as discussed in section I. Furthermore, while the improved AARBP and AARBV approaches managed to keep the voltage within the safe limits in almost all scenarios, AARC [7] failed to do so in 213 out of 1000 operating points. We exclude these infeasible results from the average results shown in Fig. 5.

Fig. 6 shows the maximum difference in line loading between different control schemes and the optimal scheme. To conduct the comparison, first we calculate the loading on each line (the line current as a percentage of the line rating). Then, we obtain the maximum difference between the loadings for each technique and the optimal approach. We can see that on average AARBP and AARBV act closer to the optimal approach. Incremental droop-based control increases the line

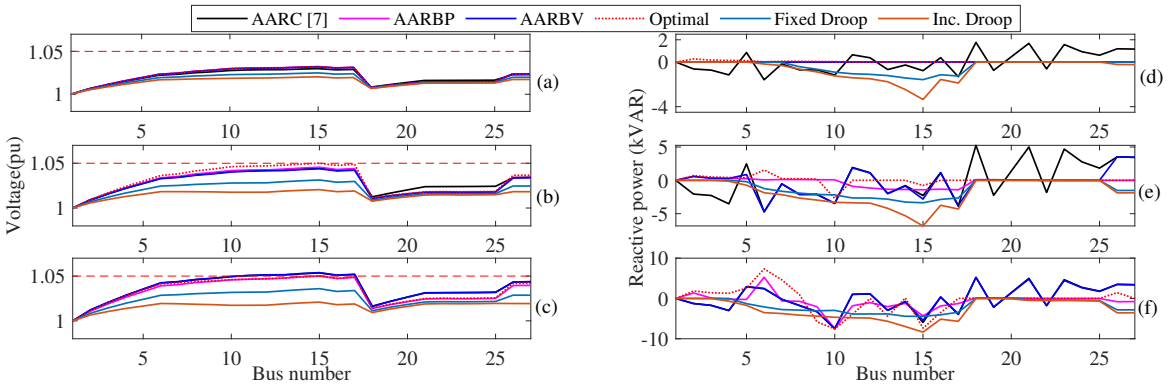

Fig. 3. Voltage magnitude and reactive power of buses in the three cases, under different Volt/Var control. (a), (b) and (c) show the voltage magnitude in *Case 1*, *Case 2* and *Case 3*, respectively. Also, (d), (e) and (f) show the reactive power in *Case 1*, *Case 2* and *Case 3*, respectively. Note that as described in text (a) and (d) AARBP and AARBV lie completely on top of each other. Also, in (c) and (d) and AARC [7] are almost on top of each other.

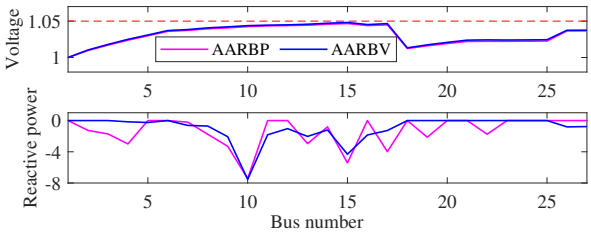

Fig. 4. Voltage profile and reactive power of buses under improved versions of AARBP and AARBV in *Case 3*.

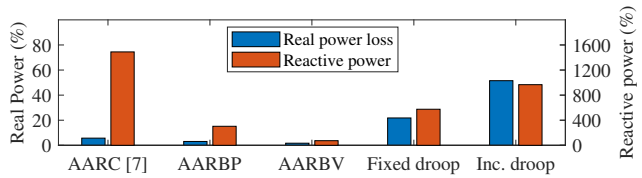

Fig. 5. Average relative difference in real power loss and inverter reactive power usage (absorption or injection) between different voltage control schemes and the optimal scheme over 1000 operating points in the 27-bus system.

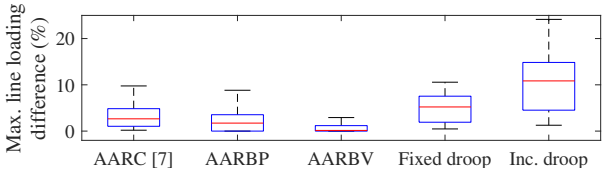

Fig. 6. Distribution of the maximum line current differences in the 27-bus system, using different approaches with the optimal scheme. On each box, the central mark indicates the median, and the bottom and top edges of the box indicate the 25th and 75th percentiles, respectively.

TABLE I
SUMMARY OF THE SIMULATION RESULTS IN THE 27-BUS SYSTEM

Control technique	Agg. real power loss (MW)	Agg. reactive power usage (MVAR)	No. voltage violation
AARC [7]	1.286	30.876	213
AARBP	1.254	7.834	1
AARBV	1.237	2.284	0
Fixed droop	1.481	13.116	4
Inc. droop	1.843	20.728	0
Optimal	1.263	1.943	0

currents more than other techniques, with droop-based control and AARC [7] behind it.

From the reported simulations we can conclude that even though purely local approaches (i.e., droop-based and incremental droop-based controls) eliminate the need for communication, they significantly increase the reactive power usage as well as the real power losses, and may create line congestion in heavily loaded lines. Other approaches investigated in this paper require a communication infrastructure and system configuration information. In particular, AARC [7] leads to an excessive use of reactive power which not only might not be able to keep the voltage within the safe limits, but also might create line congestion. On the other hand, AARBP and AARBV could keep the voltage within the safe limits in almost all the investigated operating points, with AARBV having the best performance (almost similar to the optimum yet an unachievable case). A summary of the simulation results is reported in Table I.

VI. SCALING TO A LARGE LV SYSTEM

We implement our models on a modified version of the IEEE European low voltage test feeder [32], which consists of 906 nodes and 55 residential loads. We model a balanced per-phase version of the network by connecting all residential loads to phase *A*, and a high PV penetration scenario by pairing each load with a 6 kW PV system. To generate load patterns, we first randomly choose 55 load shapes from the IEEE 906-bus 1-min resolution data. Then, we select 50 random minutes (the same minutes for every household) between 10 AM and 2 PM. Each selected minute is simulated for 20 scenarios where in each scenario, we randomly set the PV output to a value in the range 0 to 6 kW.

Fig. 7 shows the average relative difference in real power loss and reactive power usage between the optimal solution and the other approaches, over the combined thousand scenarios. We can see that similarly to the results that we obtained for the smaller 27-bus system, our proposed approaches use

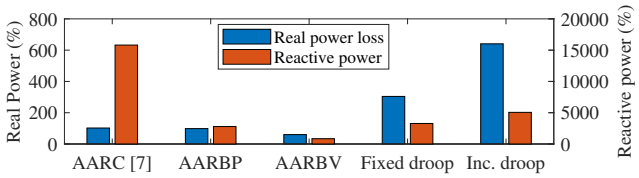

Fig. 7. Average relative difference in real power loss and inverter reactive power usage (absorption or injection) between different voltage control schemes and the optimal scheme over 1000 operating points in the 906-bus system.

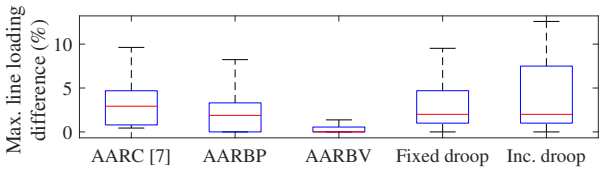

Fig. 8. Distribution of the maximum line current differences in the 906-bus IEEE system, using different approaches with the optimal scheme.

significantly less reactive power and manage to decrease real power loss compared to the other techniques. The simulation results are summarized in Table II. Note that due to the limited available reactive power (inverter size is assumed to be 10 KVA), in three scenarios, voltage violation happens in the optimal approach, indicating that the Volt/Var problem in these scenarios has no solution. Also, we can see that the Inc. droop approach manages to keep the voltage inside the limit in few more scenarios than AARBP and AARBV, but at the cost of a significant increase in real power loss and reactive power usage.

The maximum difference in line loading between different control schemes and the optimal are shown in Fig. 8. The results agree with the previous section, indicating that, on average, AARBP and AARBV leads to line loadings that are closer to the optimal. Note that since the IEEE 906-bus test system does not provide details about the ampacity of the lines, we used the following approach to obtain a sensible value for each line. First, we calculate the maximum line loading of each line over the whole day; and then we assume each line's ampacity to be three times this amount.

Furthermore, to investigate the scalability of the control schemes, we checked the connection of 10, 25, and 55 loads to the system. Table III shows the computing time for solving AARC in the three schemes using *Gurobi* [29]. The simulations are carried out on a Dell Latitude 7490 having 1.9 GHz Intel Core i5 processor with a memory of 8 GB.

VII. Conclusion

We proposed two affinely adjustable robust counterparts, that respond to changes in local real power (AARBP) and voltage magnitude (AARBV), respectively. In these approaches we directly incorporated the voltage limit constraints into a AARC of the Volt/Var problem. Through numerical simulations we show that our proposed approaches can keep the voltages inside the accepted limits for a wider range of scenarios compared to alternative approaches, while significantly decrease the reactive power usage, real power loss, and line congestion.

TABLE II
Summary of the simulation results in the 906-bus system

Control technique	Agg. real power loss (MW)	Agg. reactive power usage (MVAR)	No. voltage violation
AARC [7]	0.346	35.841	84
AARBP	0.340	6510	8
AARBV	0.274	2.132	6
Fixed droop	0.693	7.612	11
Inc. droop	1.269	11.614	5
Optimal	0.171	225	3

TABLE III
Computing time in the 906-bus test system

Number of Loads	Time(s)		
	AARC [7]	AARBP	AARBV
10	0.442	0.661	1.331
25	1.613	2.038	5.269
55	7.640	4.225	24.663

Moreover since these functions are developed in accordance with different grid codes, they are practical to implement for wide range of operating distribution systems. A further extension to our work would be to add real power curtailment to the control approach. As there are situations that due to limited reactive power available, it is not possible to keep the voltages inside the limits using only reactive power of the residential inverters.

References

[1] S. Hashemi and J. Østergaard, "Efficient control of energy storage for increasing the PV hosting capacity of LV grids," *IEEE Transactions on Smart Grid*, vol. 9, no. 3, pp. 2295–2303, 2016.

[2] M. Zeraati, M. E. H. Golshan, and J. M. Guerrero, "Distributed control of battery energy storage systems for voltage regulation in distribution networks with high PV penetration," *IEEE Transactions on Smart Grid*, vol. 9, no. 4, pp. 3582–3593, 2016.

[3] H. Zhu and H. J. Liu, "Fast local voltage control under limited reactive power: Optimality and stability analysis," *IEEE Transactions on Power Systems*, vol. 31, no. 5, pp. 3794–3803, 2015.

[4] S. Abadi, M. Mahmoodi, P. Scott, L. Blackhall, and S. Thiebaux, "Active management of LV residential networks under high PV penetration," in *2019 IEEE Milan PowerTech*. IEEE, 2019, pp. 1–6.

[5] D. K. Molzahn, F. Dörfler, H. Sandberg, S. H. Low, S. Chakrabarti, R. Baldick, and J. Lavaei, "A survey of distributed optimization and control algorithms for electric power systems," *IEEE Transactions on Smart Grid*, vol. 8, no. 6, pp. 2941–2962, 2017.

[6] H. J. Liu, W. Shi, and H. Zhu, "Decentralized dynamic optimization for power network voltage control," *IEEE Transactions on Signal and Information Processing over Networks*, vol. 3, no. 3, pp. 568–579, 2016.

[7] R. A. Jabr, "Robust volt/var control with photovoltaics," *IEEE Transactions on Power Systems*, vol. 34, no. 3, pp. 2401–2408, 2019.

[8] H. S. Bidgoli and T. Van Cutsem, "Combined local and centralized voltage control in active distribution networks," *IEEE Transactions on Power Systems*, vol. 33, no. 2, pp. 1374–1384, 2017.

[9] Y. Xu, Z. Y. Dong, R. Zhang, and D. J. Hill, "Multi-timescale coordinated voltage/var control of high renewable-penetrated distribution systems," *IEEE Transactions on Power Systems*, vol. 32, no. 6, pp. 4398–4408, 2017.

[10] R. A. Jabr, "Linear decision rules for control of reactive power by distributed photovoltaic generators," *IEEE Transactions on Power Systems*, vol. 33, no. 2, pp. 2165–2174, 2017.

[11] A. Ben-Tal, A. Goryashko, E. Guslitzer, and A. Nemirovski, "Adjustable robust solutions of uncertain linear programs," *Mathematical programming*, vol. 99, no. 2, pp. 351–376, 2004.

[12] A. Attarha, P. Scott, and S. Thiébaux, "Affinely adjustable robust admm for residential DER coordination in distribution networks," *IEEE Transactions on Smart Grid*, 2019.
[13] D. G. Photovoltaics and E. Storage, "IEEE standard for interconnection and interoperability of distributed energy resources with associated electric power systems interfaces."
[14] M. Farivar, X. Zho, and L. Che, "Local voltage control in distribution systems: An incremental control algorithm," in *2015 IEEE International Conference on Smart Grid Communications (SmartGridComm)*. IEEE, 2015, pp. 732–737.
[15] S. Uebermasser, C. Groiss, A. Einfalt, N. Thie, M. Vasconcelos, J. Helguero, H. Laaksonen, and P. Hovila, "Requirements for coordinated ancillary services covering different voltage levels," *CIRED-Open Access Proceedings Journal*, vol. 2017, no. 1, pp. 1421–1424, 2017.
[16] E. Troester, "New German grid codes for connecting PV systems to the medium voltage power grid," in *2nd International workshop on concentrating photovoltaic power plants: optical design, production, grid connection*, 2009, pp. 1–4.
[17] A. Miller, R. Strahan, S. Mcnab, T. Crownshaw, S. Pandey, N. Watson, S. Lemon, and A. Wood, "Guideline for the connection of small-scale inverter based distributed generation: An introduction and summary," 2016.
[18] W. H. Kersting, *Distribution system modeling and analysis*. CRC press, 2006.
[19] M. S. Alvarez-Alvarado, C. D. Rodríguez-Gallegos, and D. Jayaweera, "Optimal planning and operation of static var compensators in a distribution system with non-linear loads," *IET Generation, Transmission & Distribution*, vol. 12, no. 15, pp. 3726–3735, 2018.
[20] M. N. Bhukya, V. R. Kota, and S. R. Depuru, "A simple, efficient, and novel standalone photovoltaic inverter configuration with reduced harmonic distortion," *IEEE Access*, vol. 7, pp. 43 831–43 845, 2019.
[21] L. S. Xavier, A. F. Cupertino, J. T. de Resende, V. F. Mendes, and H. A. Pereira, "Adaptive current control strategy for harmonic compensation in single-phase solar inverters," *Electric Power Systems Research*, vol. 142, pp. 84–95, 2017.
[22] S. Corsi, *Voltage control and protection in electrical power systems: from system components to wide-area control*. Springer, 2015.
[23] S. Corsi, "Wide area voltage regulation protection," in *2009 IEEE Bucharest PowerTech*, 2009, pp. 1–7.
[24] S. Corsi and N. Martins, "Coordinated voltage control in transmission systems," *CIGRE Technical Brochure, Task Force*, vol. 38, p. 23, 2005.
[25] B. Perera, P. Ciufo, and S. Perera, "Advanced point of common coupling voltage controllers for grid-connected solar photovoltaic (PV) systems," *Renewable energy*, vol. 86, pp. 1037–1044, 2016.
[26] V. C. Gungor, D. Sahin, T. Kocak, S. Ergut, C. Buccella, C. Cecati, and G. P. Hancke, "Smart grid technologies: Communication technologies and standards," *IEEE transactions on Industrial informatics*, vol. 7, no. 4, pp. 529–539, 2011.
[27] M. Farivar and S. H. Low, "Branch flow model: Relaxations and convexification—part i," *IEEE Transactions on Power Systems*, vol. 28, no. 3, pp. 2554–2564, 2013.
[28] Z. Zhang, L. F. Ochoa, and G. Valverde, "A novel voltage sensitivity approach for the decentralized control of dg plants," *IEEE Transactions on Power Systems*, vol. 33, no. 2, pp. 1566–1576, 2017.
[29] L. Gurobi Optimization, "Gurobi optimizer reference manual," 2020.
[30] G. P. McCormick, "Computability of global solutions to factorable nonconvex programs: Part i—convex underestimating problems," *Mathematical programming*, vol. 10, no. 1, pp. 147–175, 1976.
[31] P. M. Castro, "Tightening piecewise mccormick relaxations for bilinear problems," *Computers & Chemical Engineering*, vol. 72, pp. 300–311, 2015.
[32] IEEE European low voltage test feeder. [Online]. Available: https://site.ieee.org/pes-testfeeders/resources.